Mixing and Phase Hold-Ups Variations Due to Gas Production in Anaerobic Fluidized-Bed Digesters: Influence on Reactor Performance

Pierre Buffière,[1] Christian Fonade,[2] René Moletta[3]

[1]Chargé de Recherche, Institut National de la Recherche Agronomique, Laboratoire de Biotechnologie de l'Environnement, Avenue des Etangs, 11100 Narbonne, France; telephone: +33-4-68-42-51-68; fax: +33-4-68-42-51-60; e-mail: buffiere@ensam.inra.fr
[2]Institut National des Sciences Appliquées de Toulouse, Laboratoire de Génie Biochimique et Alimentaire, Complexe Scientifique de Rangueil, Toulouse, France
[3]Directeur de Recherche, Institut National de la Recherche Agronomique, Laboratoire de Biotechnologie de l'Environnement, Narbonne, France

Received 5 September 1997; accepted 23 February 1998

Abstract: The influence of mixing and phase hold-ups on gas-producing fluidized-bed reactors was investigated and compared with an ideal flow reactor performance (CSTR). The liquid flow in the anaerobic fluidized bed reactor could be described by the classical axially dispersed plug flow model according to measurements of residence time distribution. Gas effervescence in the fluidized bed was responsible for bed contraction and for important gas hold-up, which reduced the contact time between the liquid and the bioparticles. These results were used to support the modeling of large-scale fluidized-bed reactors. The biological kinetics were determined on a 180-L reactor treating wine distillery wastewater where the overall total organic carbon uptake velocity could be described by a Monod model. The outlet concentration and the concentration profile in the reactor appeared to be greatly influenced by hydrodynamic limitations. The biogas effervescence modifies the mixing characteristics and the phase hold-ups. Bed contraction and gas hold-up data are reported and correlated with liquid and gas velocities. It is shown that the reactor performance can be affected by 10% to 15%, depending on the mode of operation and recycle ratio used. At high organic loading rates, reactor performance is particularly sensitive to gas effervescence effects. *Biotechnol Bioeng* **60**: 36–43, 1998.
Keywords: anaerobic fluidized bed; hydrodynamics; biogas production; kinetics; model

INTRODUCTION

Over the past 15 years, anaerobic digesters have become more and more efficient for wastewater treatment. This is mainly due to the appearance of high-rate reactors, such as the anaerobic filter (AF), the up-flow anaerobic sludge bed (UASB), and the anaerobic fluidized-bed reactor (AFBR) (Aivasidis and Wandrey, 1988; Young and McCarty, 1969). Among these three processes, the most efficient today is the AFBR (Heijnen et al., 1989). At the industrial scale, it can work under very high loading rates, up to 40 kg COD m^3 d^{-1} (Heijnen et al., 1989). Laboratory and semi-industrial scale studies reveal that treatment capacity can reach more than 100 kg COD m^{-3} d^{-1} when using an automatic control device (Ehlinger et al., 1994; Moletta and Raynal, 1992; Steyer et al., 1996). The upper limit has not yet been clearly defined. But, it seems obvious that, above a certain loading rate, the limitations of the process are not only biological. The hydrodynamics in the reactor, such as mass transfer, biogas effervescence, or liquid mixing may be at the origin of these problems. The aim of this study is to investigate the different aspects of hydrodynamics in fluidized-bed reactors and, especially, the effect of biogas effervescence. First, we detail their nature and possible effects. We then examine experimental results showing the main properties of the AFBR toward the flow pattern. Finally, we develop a modeling approach to account for gas production effects in the scale-up of these systems.

In anaerobic fluidized-bed reactors, liquid mixing is commonly described by a perfectly mixed model. This is mostly due to the fact that those reactors are operated under very high recycling ratios (over 20), at least during the start-up period: The support material, not colonized, is more difficult to fluidize and the input flow rate is low because the organic load is not high enough (Fitzgerald, 1996; Prakash and Kennedy, 1996). However, most of the reactors are subject to high bed expansion following biofilm growth on the granular carrier and the fluidization flow has to be reduced to avoid particle elutriation. During the same time, the input flow rate is increased to follow the treatment capacity of the process. Both actions result in a decrease of the recycle ratio and the perfectly mixed model hypothesis may no longer be valid. Recent investigations have proposed that the axially dispersed plug flow model could be used as a model for anaerobic fluidized-bed reactors, but this study

Correspondence to: P. Buffière

 CCC 0006-3592/98/010036-08

did not take into account the effect of biogas production (Davison, 1989). The importance of gas production in biological beds has never been investigated in a systematic manner. Some have compared two-phase systems and triphasic reactors and considered that gas-producing reactors could be described by the same approach as classical triphasic reactors (Turan and Öztürk, 1996). It has also been observed that, in a yeast bed of *Saccharomyces cerevisiae* flocs, gas effervescence could lead to considerable changes in axial dispersion (Gommers et al., 1986). Unfortunately, no details were available concerning the gas flow rate produced and its influence on axial dispersion. Gas-producing biological beds are seldom considered real triphasic reactors, and concern rather ethanol fermentation (Brohan and McLoughlin, 1984; Webb et al., 1996). These investigators have modified the classical correlation to adapt it to the gas flow gradient in the reactor. This seems to be a rather good approximation if the gas phase has the same behavior (bubble size and velocity) in gas-producing and in gas-injected systems. In the case of anaerobic digestion, the common belief is to ignore the gas production effect. Nevertheless, the bed contraction phenomenon due to gas introduction is well known in classical three-phase fluidized beds when small and/or dense particles are used (Fan, 1989). Investigations on this subject have shown interesting results concerning bed height, which seemed not much affected by the biogas (Diez-Blanco et al., 1995). In this study, the contraction phenomenon due to biogas production in a fluidized bed 6 m in height was estimated to be less than 6%. Based on this result, the investigators considered the effect of biogas on the hydrodynamic behavior negligible. This may be true for the bed height, but certainly not for the phase hold-ups and liquid mixing. If we take this example, and if we assume that liquid and solid hold-ups are equal to 0.5 without gas and gas hold-up is equal to 0.05 with gas, a 6% contraction leads to a solid hold-up of 0.532 and a liquid hold-up of 0.418. This represents a dramatic drop in the contact time between liquid and solid of more than 16%, which directly affects reactor performance. For all these reasons, knowing the effect of hydrodynamics in gas-producing fluidized beds is a key point for further design and scale-up of anaerobic fluidized beds.

MATERIALS AND METHODS

Hydrodynamic Study

Hydrodynamic study was carried out on a fluidized bed without biomass in which an in situ gas production system was adapted. The apparatus consisted of a tubular column of 1.5 m height and 0.115 m diameter, with a calming section at its top (Fig. 1). The liquid phase was recycled with a centrifugal pump to ensure fluidization. Gas generation was performed by chemical reaction between sulfuric acid and sodium bicarbonate. The liquid medium was an aqueous solution of sulfuric acid (0.5% w/w). Saturated bicarbonate was introduced through eight ports evenly distributed along

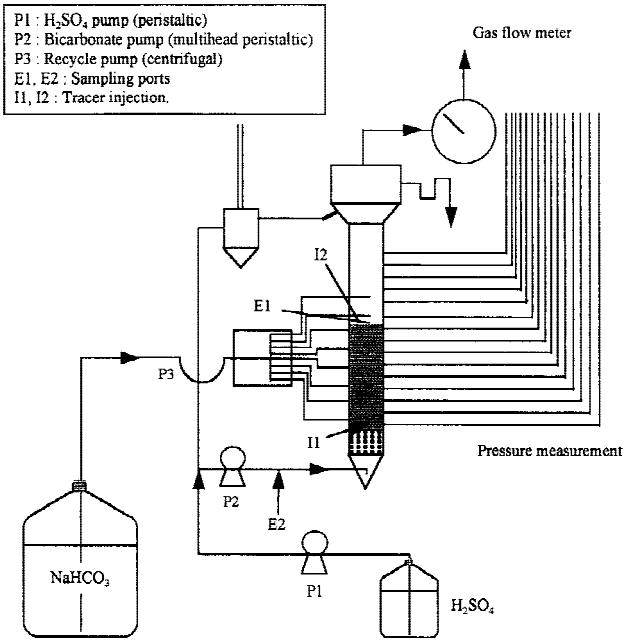

Figure 1. Experimental device for the hydrodynamic studies.

the bed height to simulate biogas production. The bicarbonate flow rate was adjusted to obtain the desired gas production flow rate. Static pressure measurements allowed determination of the phase hold-ups by Eqs. (1), (2), and (3), representing the expression of bed weight versus pressure gradient, relation between hold-ups, and direct measurement of solid hold-up, respectively. In the equations, ϵ_i are the hold-ups, ρ_i the densities (kg m^{-3}), g the acceleration of gravity (m s^{-2}), and M_s the mass of the solid (Fan, 1989; Wild et al., 1984).

$$\frac{dp}{dz} = (\varepsilon_l \rho_l + \varepsilon_s \rho_s + \varepsilon_g \rho_g) g \tag{1}$$

$$\varepsilon_l + \varepsilon_s + \varepsilon_g = 1 \tag{2}$$

$$\varepsilon_s = \frac{M_s}{\rho_s A_c H} \tag{3}$$

RTD measurements in the bed were done using the tracer injection method. The tracer was lithium chloride. After injection in the bottom of the reactor, samples were taken every 10 seconds above the bed and lithium concentrations were measured with a flame photometer. The RTD could then be calculated from the lithium concentration according to Eq. (4), where $E(t)$ is the RTD function (h^{-1}), $C(t)$ the lithium concentration (kg m^{-3}), C_i the concentration of the ith sample, and Δt_i the sampling interval. Axial dispersion coefficients were determined according to Levenspiel (1972), using the open vessel model with *through-the-wall* measurements:

$$E(t) = \frac{C(t)}{\int_0^\infty C(t)dt} \cong \frac{C_i}{\sum_i C_i \Delta t_i} \tag{4}$$

The system could also function as a real three-phase reactor, because a gas diffuser was adapted at the bottom of the bed. This adaptation was very useful for comparison of the behavior of the bed with injected gas or with generated gas, because it could be related to previous investigations on three-phase fluidized beds (Fan, 1989; Wild et al., 1984).

Compared with a real bioreactor, this configuration presents the great advantage of being easily adaptable to desired operating conditions without delay. Consequently, systematic studies could be done with repeatability tests, which could not be performed with a real AFBR. Our experiments focused on the influence of gas and liquid velocity on gas hold-up and liquid mixing in the fluidized zone.

Biological Kinetics

The model used for the kinetics of anaerobic digestion was determined experimentally on a 0.18-m^3 fluidized bed (see Fig. 2) treating concentrated wine distillery wastewaters (12 $g_{TOC}\ L^{-1}$). This reactor was operated at high recycle ratio (40 to 100) using the steady-state values of effluent concentration and TOC removal velocity (r_{TOC}) defined by Eq. (5), where τ is the hydraulic retention time in the fluidized bed:

$$r_{COT} = \frac{TOC_{in} - TOC_{out}}{\tau} \tag{5}$$

Model Development

The general expression of a dispersed plug flow model can be used to describe the mass balance in a biological fluidized-bed reactor in steady state:

$$E_{zl}\frac{d^2S}{dz^2} = \frac{U_1}{\varepsilon_1}\cdot\frac{dS}{dz} + r_{max}\frac{S}{K_s + S} \tag{6}$$

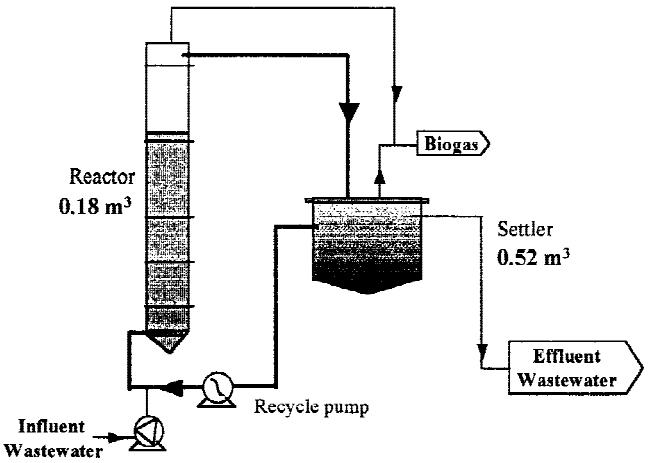

Figure 2. Anaerobic fluidized-bed reactor treating wine distillery wastewater.

With Dankwerts conditions expressed as follows:

$$z = 0,\ U_1S_0^- = U_1S_0^+ - \varepsilon_1E_{zl}\frac{dS}{dz}$$

$$z = H,\ \frac{dS}{ds} = 0$$

S_0^- is the value of substrate concentration entering the reactor. It is equal to the inlet concentration, S_{in}, when no recycle is applied. Otherwise, it is expressed as:

$$S_0^- = \frac{S_{in} + RS_{out}}{R+1}$$

In reduced coordinates, the mass balance equation converts to:

$$\frac{1}{Pe}\frac{d^2s}{dx^2} = \frac{ds}{dx} + Da\frac{s}{l+s} \tag{7}$$

with the following notations:

$$x = \frac{z}{H},\ s = \frac{S}{K_s},\ Da = \frac{r_{max}}{K_s}\cdot\frac{H\varepsilon_l}{U_l} \text{ and } Pe = \frac{U_lH}{\varepsilon_lE_{zl}}$$

This model can be solved, for instance, by using a finite difference method once the parameters (*R*, *Pe*, *Da*) are fixed. Nevertheless, we have seen that gas production strongly influences those parameters. First, the bed height, *H*, is modified when gas is generated through the contraction effect. Second, the values of *Pe* and ϵ_l also depend on the gas flow rate. Finally, the gas flow rate can only be calculated from model resolution because it is linked to TOC conversion (to simplify the model, we considered that 1 kg of TOC consumed resulted in 0.24 m^3 of biogas under STP conditions, which in our case corresponds to 0.6 m^3 of biogas per kilogram of COD). To conclude, the model resolution requires parameters having values that depend on the solution. Therefore, an iterative procedure has been developed to solve the problem. This procedure is summarized by the algorithm depicted on Figure 3. The input data are the reactor volume (height, diameter), the unexpanded bed height, the input flow rate and TOC concentration, the liquid velocity in the reactor (and thus the liquid recycle flow rate), and the characteristics of the support material (terminal velocity, expansion index, particle diameter). The aim of the program is thus to estimate the outlet concentration of the reactor. Because it is an iterative procedure, it requires an initialization step. It is performed by estimating the outlet concentration under perfectly mixed liquid-phase conditions (i.e., the CSTR model) without taking into account the gas production effect. In this step, the program uses the Richardson and Zaki correlation to estimate the liquid hold-up in the two-phase fluidized bed (ϵ_{l0}). Then, the outlet concentration is found by solving the mass balance with the CSTR model:

$$S_{in} - S_{out} = \tau\cdot r_{max}\frac{S_{out}}{K_s + S_{out}},\ \text{with } \tau = \frac{\varepsilon_{10}V}{q_{in}}$$

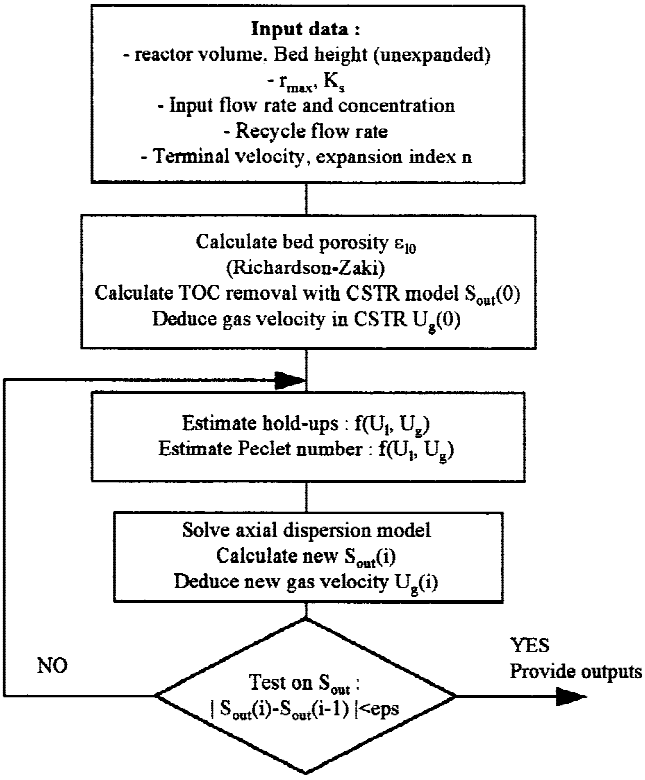

Figure 3. Iterative procedure for gas-producing fluidized-bed performance calculation.

Thus:

$$S_{out} = \frac{-(K_s - S_{in} + \tau r_{max}) + \sqrt{(K_s - S_{in} + \tau r_{max})^2 + 4K_s S_{in}}}{2} \tag{8}$$

At this point, the program enters the loop and estimates the biogas flow rate produced under these conditions. It computes the new values of hold-ups and Peclet numbers in the three-phase fluidized bed according to the correlations found from the experimental data for the phase hold-ups and the liquid mixing [see Eqs. (10), (12), and (13) in the ''RESULTS'' section]. The next step is the model resolution using a finite difference method, which leads to a new value of $S_{out.}$ This value is compared with that previously calculated. If no evolution is found, this value is taken as the solution. Otherwise, the loop continues and the program calculates the new gas flow rate, hold-ups, and Peclet number. This program was implemented on a PC with Matlab software as the computing tool. Computing takes a few seconds on a PC with a Pentium processor. In the ''RESULTS'' section, we present some simulation that can be obtained from this program. The first series of results shows a typical concentration profile in the reactor and the second is an attempt at TOC removal efficiency calculation at different organic loading rates for an industrial-scale anaerobic fluidized-bed reactor. The program also computes the results obtained with the dispersed plug flow (DPF) model only (without taking hold-up variations into account) to see which is the most relevant hydrodynamic phenomenon (liquid mixing effect or phase hold-up variations).

RESULTS AND DISCUSSION

Carbon Removal Kinetics

The total organic carbon removal kinetics are found to be in good agreement with the Monod model. The TOC uptake rate can be expressed by Eq. (9). Parameters r_{max} and K_s are found by plotting the inverse of r_{TOC} versus $1/TOC_{out}$ (Fig. 4). The value of r_{max} is 35 g_{TOC} L^{-1} h^{-1}, K_s is 1.27 g_{TOC} L^{-1}, and the determination coefficient is 0.988:

$$r_{TOC} = r_{max} \frac{S}{K_s + S} \tag{9}$$

In Eq. (9), S is the TOC concentration in the reactor (supposed perfectly mixed). This assumption is reasonable here because the reactor is working at a high recycling ratio and relatively low organic loading rate (below 40 kg COD m^{-3} d^{-1}). Hence, the effect of gas effervescence is limited in this case.

Hydrodynamics

Bed Contraction

The bed contraction phenomenon can be observed by plotting the variations of the bed porosity with gas velocity (Fig. 5). The fall of the bed porosity is all the more pronounced as the liquid velocity is high, except possibly for the smallest value of U_l in the generated gas case. To get an approximate model of this phenomenon, we found a relation between ϵ_s/ϵ_{s0} and U_g. At first approximation, this relation was found independent from the liquid velocity and could be expressed as a power low of gas velocity [Eq. (10)]:

$$\frac{\varepsilon_s}{\varepsilon_{s0}} = 1 + 0.045 U_g^{0.4} \tag{10}$$

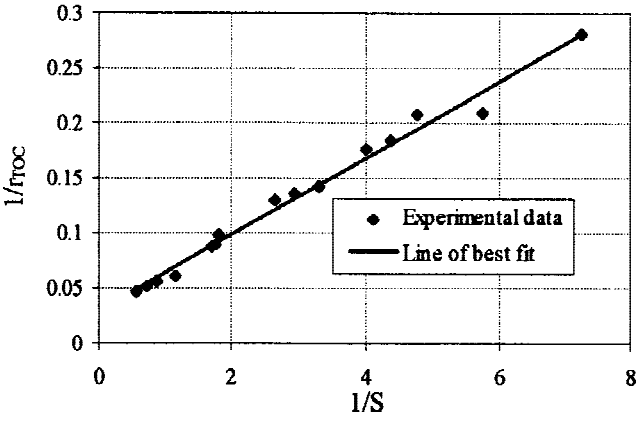

Figure 4. Monod kinetics parameter determination.

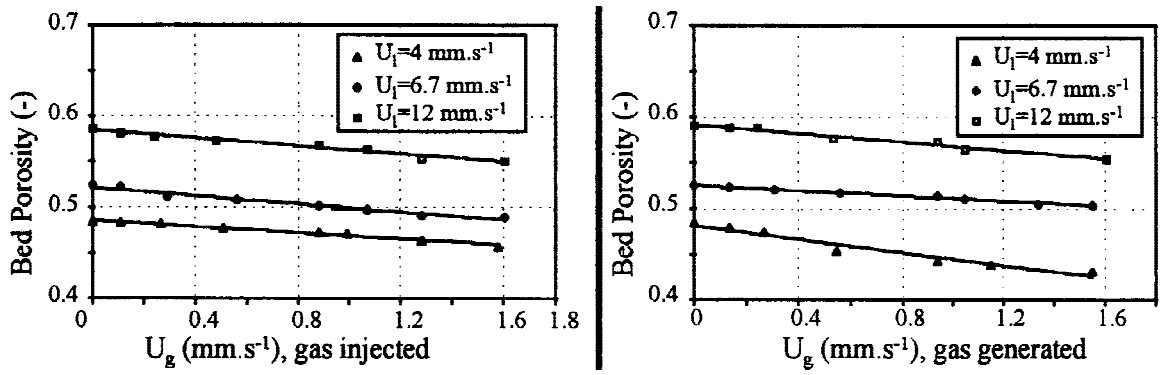

Figure 5. Influence of gas velocity on bed porosity at various liquid velocities for the two modes of gas introduction.

Gas Hold-Up

The variations of the gas hold-up with gas velocity are reported in Figure 6 with gas injected and gas generated. The major trend here is an increase of gas hold-up with gas velocity up to values of 0.035 when gas is injected, and 0.05 when gas is generated. It is striking that the gas hold-up is higher when gas is generated, in particular because the value of gas velocity is that calculated with the total gas flow, at the top of the bed. The average gas velocity all along the column is slightly lower in this case. This is explained by the difference between the bubble populations in the two cases. The influence of liquid velocity on gas hold-ups is less obvious. Pozzolana particles seem rather sensitive to liquid velocity, and gas hold-up is higher for high liquid velocity than for those lower. This can be explained by a change in the bubble flow regime (from coalesced bubble flow at low liquid velocity to dispersed bubble flow at high velocity) more than by a direct effect of liquid velocity, because it is well known that the gas hold-ups in coalescing bubble flow are lower than in dispersed bubble flow (Fan, 1989).

As the effect of liquid flow rate is difficult to relate to the measured values of ϵ_g, we tried to find a direct relation between gas flow rate and gas hold-up. Because we did not study the variations of the column diameter, we could find only the values of the coefficient of U_g and we supposed that the coefficient of d_p was 0.168, as proposed by Begovich and Watson (1978):

For gas injected:

$$\varepsilon_g = (8.66 \pm 0.05) d_p^{0.168} U_g^{0.69} \ (r^2 = 0.91, 60 \text{ points}) \tag{11}$$

For gas generated:

$$\varepsilon_g = (13 \pm 1.2) d_p^{0.168} U_g^{0.7} \ (r^2 = 0.85, 60 \text{ points}) \tag{12}$$

Liquid Mixing

Among the range of gas and liquid velocities studied here, the axially dispersed plug flow model was found to provide an accurate description of the liquid mixing in the fluidized-bed reactor. An example of tracer pulse response is presented on Figure 7, and reveals good agreement between the experimental data and the model. What can be seen in this plot is that the degree of mixing in the bioreactor is relatively high, and low column Peclet numbers are found (between 1.4 and 4).

For modeling purposes, knowing the variations of the Peclet number of axial dispersion coefficient is necessary. Therefore, several correlations were tested to support our experimental determination of E_{zl}. Among those available

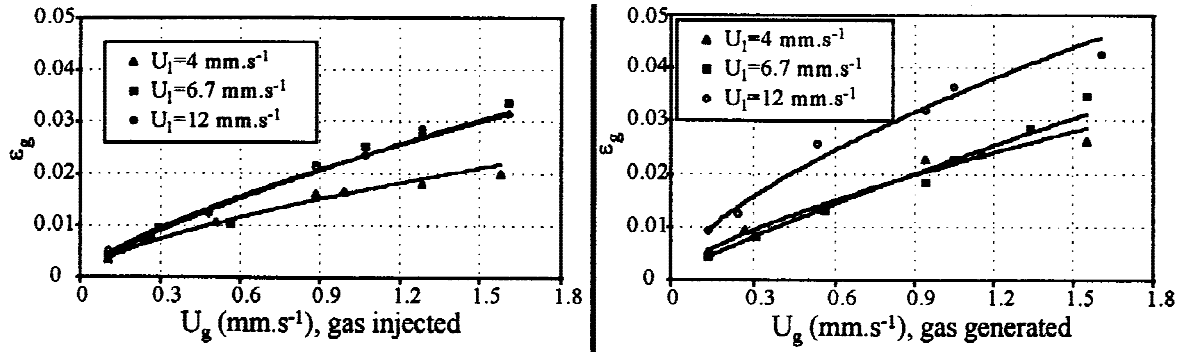

Figure 6. Influence of gas velocity on gas hold-up for the two modes of gas introduction.

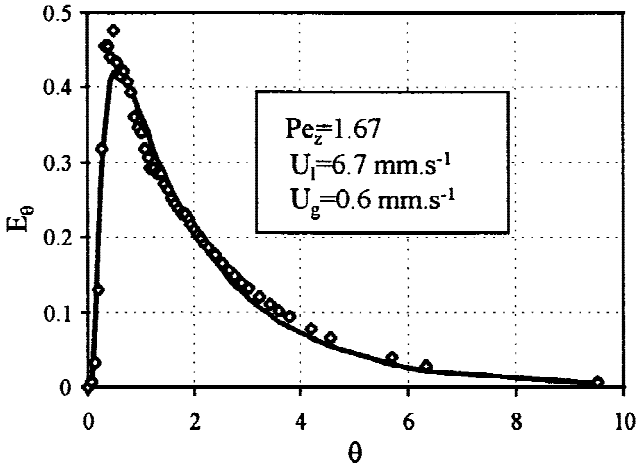

Figure 7. Example of experimental pulse response and corresponding axial dispersion model.

in the literature, the correlation of Muroyama et al. (from Fan, 1989) was found to be the most appropriate and gave a correct fit to our experimental data (see Table I). This correlation is an expression of a modified Peclet number (calculated with the column diameter as space length parameter) as a function of liquid and gas velocities and column diameter.

$$\frac{D_c U_l}{\varepsilon_1 E_z} = 1.01 U_l^{0.738}\, U_g^{-0.167}\, D_c^{-0.583} \qquad (13)$$

Simulation Results

Example of Calculation and Concentration Profile in the Reactor

Using Eqs. (10) and (12) for predicting hold-ups in the three-phase fluidized bed, and Eq. (13) for the axial dispersion coefficient, it is thus possible to use the algorithm to predict the reactor performance under any operational condition. In the following example, the concentration profile plotted on Figure 8 has been obtained. It is noticeable that, despite a significant recycle ratio ($R = 6$), the concentration decreases between the bottom and the top of the bed are not negligible (from 0.12 to 0.09 kg COT m^{-3}). Otherwise, the outlet concentration computed from the model is not different from that obtained with the CSTR model. Typical of the results commonly obtained is that the conversion is lower with the dispersed plug flow model taking the hold-ups into account than with the CSTR. This is in fact due only to the decrease in the contact time resulting from bed contraction and gas hold-up, as will be shown in what follows.

This can be seen more clearly in Figure 9, which shows the influence of organic loading rate (expressed in kg COD m^{-3} d^{-1}) on the performance of a 10-m reactor with a 2-m internal diameter. Three series of computed data are plotted: the TOC conversion obtained with the CSTR model; the conversion that would be obtained with the dispersed plug flow model without taking the hold-up variations into account; and the conversion estimated with the complete model. As expected, the conversion calculated without taking the hold-up variations into account is better than for a CSTR. This is quite natural because the dispersed plug flow reactor is more efficient than a perfectly mixed system due to the reaction order (above 0, no inhibition). Thus, as the complete model gives a lower value than the CSTR, it is only due to the effect of bed contraction and gas hold-up that there are reductions in contact time between the reactive phases and thus the mean residence time of the liquid in the bed. As expected, the mixing of the liquid phase has a slight influence on reactor performance because it is very close to a mixed system. This is all the more true for large-scale reactors in which the degree of axial dispersion is amplified by the increase in column diameter.

CONCLUSIONS

This article is composed of an experimental and a modeling section on the gas-producing fluidized bed. In the experi-

Table I. Axial dispersion coefficient at different gas and liquid velocities.

		E_{zl} (cm^2 s^{-1})		
U_g (mm s^{-1})	U_l (mm s^{-1})	Experimental	Muroyama et al. (Fan, 1989)	ΔE (%)
0.27	4.0	39.85	41.52	4.04
0.53	4.0	44.17	48.16	8.30
0.83	4.0	43.15	53.70	19.65
1.07	4.0	52.59	57.70	8.85
0.29	6.7	33.32	43.45	23.31
0.51	6.7	28.57	48.31	40.86
0.80	6.7	56.53	53.23	6.19
1.18	6.7	59.62	58.30	2.26
0.27	12	42.76	44.79	4.53
0.40	12	38.01	48.49	21.62
0.53	12	62.67	51.48	21.73
				Mean (%) = 14.67

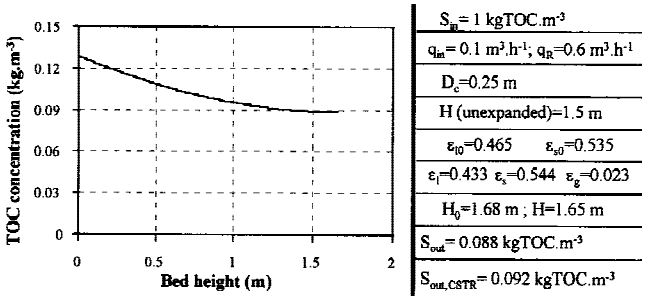

Figure 8. Example of calculation and concentration profile.

mental section, we obtained the main hydrodynamic characteristics of gas-producing beds (axial dispersion and hold-ups) and correlations for their estimation. These include:

- Over the range of gas and liquid velocities studied, the bed contraction effect was found to depend on gas velocity only.
- The gas hold-up could also be described by a direct correlation, depending on biogas velocity.
- The degree of axial mixing was found to be in rather good agreement with the correlation of Muroyama et al. (Fan, 1989).
- The model proposed here accounts for all different effects of biogas production and allows computation of the performance of a gas-producing bioreactor once the biological kinetics is determined. It was applied to the particular case of anaerobic treatment of wine distillery wastewaters. Because the value of the gas velocity is needed to determine the hydrodynamic parameters of the bed, an iterative procedure was developed.

The effect of hydrodynamics, and particularly of biogas production, in upflow-fluidized beds was found to be of two different kinds:

- First, gas production modifies the degree of axial mixing, which is responsible from the establishment of a concentration gradient in the reactor. This effect is attenuated by scaling up the reactor size, but may be particularly important for reactors operating at low recycle ratios (for higher recycle ratios, the perfectly mixed model can be used as a first approximation).
- Second, gas production is responsible from bed contraction, which reduces the contact between the liquid and the bioparticles. This effect is the most pronounced and, consequently, it may reduce the overall efficiency of the reactor. This effect is amplified by scaling up, because for large-scale fluidized beds the gas velocity can reach high values (close to liquid velocity).

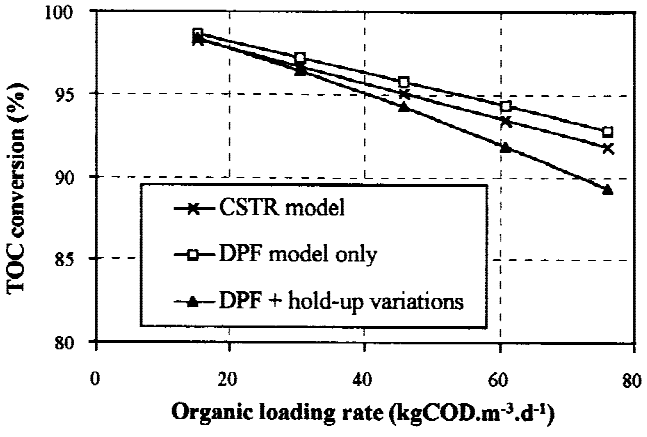

Figure 9. Influence of organic loading rate on reactor performance. Reactor diameter: 2 m; initial bed height: 10 m; inlet concentration 1 kg_{TOC} m^{-3} (2.5 kg_{COD} m^{-3}).

NOMENCLATURE

A_c	cross-sectional area of the column (m^2)
$C(t)$	tracer concentration (kg m^{-3})
COD	chemical oxygen demand (kg m^{-3})
$Da = r_{max}/K_s \cdot H\epsilon_l/U_l$	Damköhler number (−)
d_p	particle diameter (m)
D_c	column diameter (m)
E_{zl}	axial dispersion (m^2 s^{-1})
$E(t)$	residence time distribution (RTD) function (s^{-1})
$E_\theta = \bar{t}(t)$	reduced RTD function (−)
g	gravitational acceleration (m^2 s^{-1})
H_0	height of liquid–solid fluidized bed
H	bed height (m)
K_s	half-saturation concentration on Monod expression (kg_{TOC} m^{-3})
M_s	mass of solid (kg)
n	expansion index (−)
$Pe_z = U_l H/\epsilon_1 Ezl$	Peclet number based on bed height (−)
q_{in}	input flow rate (m^3 h^{-1})
r_{max}	maximal reaction rate in Monod expression (kg_{TOC} m^{-3} h^{-1})
S	substrate concentration (kg_{TOC} m^{-3})
$s = S/K_s$	reduced substrate concentration (−)
TOC	total organic carbon concentration (kg m^{-3})
$\bar{t}$	mean residence time in the column (s)
U_g	gas superficial velocity (m s^{-1})
U_l	liquid superficial velocity (m s^{-1})
U_t	terminal velocity of particles (m s^{-1})
V	active reactor volume (m^3)
$x = z/H$	reduced bed height

Greek letters

ϵ	bed porosity (−)
ϵ_g	gas hold-up (−)
ϵ_l	liquid hold-up (−)
ϵ_s	solid hold-up (−)
ϵ_{l0}	liquid hold-up in the liquid–solid fluidized bed (−)
ϵ_{s0}	solid hold-up in the liquid–solid fluidized bed (−)
ρ_s	gas density (kg m^{-3})
ρ_s	solid density (kg m^{-3})
ρ_t	liquid density (kg m^{-3})
$\theta = t/\bar{t}$	reduced time (−)
$\tau = \epsilon_{10} V/q_{in}$	theoretical residence time in the active part of the reactor (h)

References

Aivasidis, A., Wandrey, C. 1988. Recent developments in process and reactor design for anaerobic wastewater treatment. Water Sci. Technol. **20**: 211–218.

Begovich, J., Watson, J. 1978. An electroconductivity technique for the measurements of axial variation of holdups in three phase fluidized beds. AIChE J. **24**: 351–354.

Brohan, B., McLoughlin, J. 1984. The influence of yeast metabolism on dispersion in a fluidized yeast bed. Appl. Microbiol. Biotechnol. **20**: 146–149.

Davison, B. H. 1989. Dispersion and holdup in a three-phase fluidized bed bioreactor. Appl. Biochem. Biotechnol. **20/21**: 449–460.

Diez-Blanco, V., Garcia-Encina, P., Fernandez-Polanco, F. 1995. Effect of biofilm growth, gas and liquid velocities on the expansion of an anaerobic fluidized bed reactor. Water Res. **29**: 1649–1654.

Ehlinger, F., Escoffier, Y., Couderc, J. P., Leyris, J. P., Moletta, R. 1994. Development of an automatic control system for monitoring and control an anaerobic fluidized bed. Water Sci. Technol. **10–11**: 289–298.

Fan, L-S. 1989. Gas–liquid–solid fluidization engineering. Butterworth, London.

Fitzgerald, P. A. 1996. Comprehensive monitoring of a fluidized bed reactor for anaerobic treatment of high strength wastewater. Chem. Eng. Sci. **51**: 2829–2834.

Gommers, P. J. F., Christoffels, L. P., Kuenen, J. G., Luyben, K. C. A. M. 1986. Gas phase influence on the mixing in a fluidized bed bioreactor. Appl. Microbiol. Biotechnol. **25**: 1–7.

Heijnen, J., Mulder, A., Enger, W., Hoeks, F. 1989. Review on the application of anaerobic fluidized bed reactors in wastewater treatment. Chem. Eng. J. **41**: B37–B50.

Levenspiel, O. 1972. Chemical reaction engineering. 2nd edition. Wiley, New York.

Moletta, R., Raynal, J. 1992. Procédés de dépollution et recherches actuelles dans le domaine vinicole. Revue Française d'œnologie **134**: 37–43.

Prakash, R., Kennedy, K. J. 1996. Kinetics of an anaerobic fluidized bed reactor using biolite carrier. Can. J. Civ. Eng. **23**: 1305–1315.

Steyer, J-P, Buffière, P., Rolland, D., Moletta, R. 1996. Contrôle d'un pilote semi-industriel de dépollution carbonée au travers d'un dialogue avec les bactéries. Revue d'Electricité et d'Electronique **7**: 88–91.

Turan, M., Öztürk, I. 1996. Longitudinal dispersion and biomass hold-up of anaerobic fluidized bed reactors. Water Sci. Technol. **34**: 461–468.

Webb, O. F., Davison, B. H., Scott, T. C. 1996. Modeling scale-up effects on a small pilot scale fluidized bed reactor for fuel ethanol production. Appl. Biochem. Biotechnol. **57/58**: 639–647.

Wild, G., Saberian, M., Schwartz, J., Charpentier, J-C. 1984. Gas–liquid–solid fluidized bed reactors: state of the art and industrial possibilities. Int. Chem. Eng. **24**: 639–678.

Young, J. C., McCarty, P. L. 1969. The anaerobic filter for waste treatment. J. Water Pollut. Control Fed. **41**: R160.